ARTICLES

Kinetics of Triplet−Triplet Annihilation of Tetraphenylporphyrin in Liquid and Frozen Films of Decanol on the External Surface of Zeolite. Fast Probe Diffusion in Monolayers and Polycrystals

Peter P. Levin,*,†,‡ Sílvia M. B. Costa,† Teresa G. Nunes,§ Luis F. Vieira Ferreira,‖ Laura M. Ilharco,‖ and Ana M. Botelho do Rego‖

Centro de Quimica Estrutural and Centro de Quimica Fisica Molecular, Complexo 1, Instituto Superior Tecnico, Av. Rovisco Pais, 1049-001 Lisbon Codex, Portugal, Departamento de Engenharia de Materiais, IST/ICTPOL, Instituto Superior Tecnico, Av. Rovisco Pais, 1049-001 Lisbon Codex, Portugal, and Institute of Biochemical Physics, Russian Academy of Sciences, ul. Kosygina 4, 117334 Moscow, Russian Federation

Received: July 16, 2002; In Final Form: October 17, 2002

The kinetics of diffusion-controlled triplet−triplet annihilation (TTA) and simultaneous delayed fluorescence (DF) of *meso*-tetraphenylporphyrin (TPP) in thin films (1−100 nm) of *n*-decanol (DEC) adsorbed on the external surface of NaA zeolite were studied by the diffuse-reflectance laser flash technique in the temperature range 220−330 K. The value of the TTA bimolecular rate constant (k_{TTA}^{L}) referred to the DEC volume in the solid samples (with the amount of DEC being ≥10 monolayers) is similar to that measured in neat DEC. At temperatures above the melting point of DEC (280 K), the decrease of the DEC film thickness to one monolayer results in 20-fold increase of k_{TTA}^{L} which is attributed to the confined reaction volume where TPP is concentrated as well as to the enhanced TPP diffusion in this volume. The DEC monolayers on the NaA external surface are vertically ordered DEC molecules with external hydrocarbon region characterized by enhanced molecular mobility confirmed by solid-state ^{1}H NMR spectra. The apparent rate of TTA in neat DEC or in bulk DEC multilayers increases by more than 1 order of magnitude with the freezing of DEC and further temperature decrease down to 260 K whereas that in DEC monolayers does not. The apparent k_{TTA}^{L} value measured far below the melting point of DEC is independent of DEC film thickness and coincides with that in neat frozen DEC which presents some organized monolayers with TPP localized in the vicinity of aliphatic chains.

Introduction

The investigation on the reactivity of molecules confined within organic layers and thin films adsorbed on solid inorganic supports is of fundamental interest since it is important in many areas of modern science and technology.[1−3] One of the useful methods which is capable of providing some insight into the molecular mobility and spatial distribution of reactants within such microreactors is the kinetic monitoring of bimolecular photoprocesses, using a laser pulse to produce phototransients and time-resolved spectroscopy to follow their decay. Among a variety of photoinitiated bimolecular reactions used to probe the microproperties of organic layers and interfaces, the triplet−triplet annihilation (TTA) is a particular one. The TTA-induced delayed fluorescence (DF) enables the use of highly sensitive fluorescent spectroscopic techniques and, therefore, it is possible to study very diluted systems with small microreactors occupying only an insignificant fraction of the sample. The TTA kinetics have been used to probe the properties of molecular environment of triplets (T) adsorbed on the porous solid surfaces,[4−7] on the surface of quantized colloidal semiconductor particles,[8] in zeolites network,[9−11] incorporated into the bilayers,[12−15] and along the conjugated polymer molecules.[16] Our recent laser flash photolysis investigation of *meso*-tetraphenylporphyrin (TPP) in thin films of *n*-decanol (DEC) covering the external surface of NaA zeolite particles demonstrated that TTA is a useful probe of fluidity and diffusional processes pointing to a supramolecular organization in organic layers on solid surfaces.[17,18]

The fundamental aspects of interfacial layers of long-chain organic molecules, in particular alcohols, at the interfaces are ordering, cluster formation, nucleation, and preferential surface crystallization (see, e.g., refs 19−25). The TTA kinetics of TPP in DEC seems to be an attractive tool to study the ordering and degree of crystallinity of DEC films. It was found that freezing of neat DEC results in dramatic acceleration of TTA due to the concentration of TPP molecules in some liquidlike domains in polycrystalline matrix.[18,26,27] Solvent crystallization (α-transition) is accompanied by the "molecular extrusion" of the dissolved substance from the nucleating crystal into the noncrystalline liquidlike defects at the interface of microcrystals.[28] Our preliminary results demonstrated that the magnitude of this effect

* Corresponding author. Centro de Quimica Estrutural, Complexo 1, Instituto Superior Tecnico, 1049-001 Lisbon, Portugal. Fax: +351 1 846 4455. E-mail: sbcosta@popsrv.ist.utl.pt.
† Centro de Quimica Estrutural.
‡ Institute of Biochemical Physics.
§ Departamento de Engenharia de Materiais.
‖ Centro de Quimica Fisica Molecular.

10.1021/jp021635i CCC: $25.00 © 2003 American Chemical Society
Published on Web 12/28/2002

in DEC films depends significantly on the amount of DEC on the NaA surface reflecting the ordering of DEC in films of molecular thickness.[18]

In the present work, we continue the previous room-temperature laser flash photolysis study of TTA kinetics of TPP focusing our attention on thin films (estimated thickness is varied in the range 1−100 nm) of DEC adsorbed on the external surface of NaA zeolite (0.4 nm molecular sieves) at the temperature range 220−330 K. Because of the emphasis on the effect of film structure, the ratio TPP/DEC was kept smaller than 0.1 mmol/L (solubility of TPP in DEC[17,26]) in order to avoid the precipitation of TPP molecules adsorbed on the solid support. The work includes other spectroscopic techniques: solid-state ^{1}H NMR, X-ray photoelectron spectroscopy (XPS), and diffuse reflectance Fourier transformed infrared (DRIFT) spectroscopy in order to obtain some evidence of the molecular organization of DEC on the zeolite surface.

Experimental Section

Materials. TPP (from Hambright, Washington, DC) was purified by recrystallization from methanol. The sodium form of zeolite A (NaA, Aldrich, $Na_{12}[(AlO_2)_{12}(SiO_2)_{12}]\times 12H_2O$, crystallite particle size 1−2 μm was controlled by electron microscopy, estimated external surface area 3 m^2/g[29,30]) was vacuum dried at 400 K for 48 h prior to use, but not handled in a dry glovebox. In this way only the physisorbed water was removed. Benzene (Aldrich, spectrophotometric grade) was dried over P_2O_5 and then used as solvent for the TPP and DEC. 1-Decanol (Fluka, puriss., mp 279.4 K) was refined by repeated freezing.

Sample Preparation. The solutions (2 mL) of TPP and DEC in benzene ([TPP]/[DEC] ≤ 0.1 mmol/L) were added to NaA samples (1 g). The suspensions were stirred during evaporation at 300 K. The final removal of benzene was achieved by heating the samples at about 300 K under vacuum of 0.1 Pa. It was found that even when 0.35 mL of DEC are loaded onto 1 g NaA the sample still holds a dry powder demonstrating the strong multilayer adsorption.[17] This DEC amount corresponds approximately to 100 monolayers (one monolayer is 4 μL/g, using a typical value 0.25 nm^2 for molecular area in DEC monolayers[21−25]). The large TPP and DEC molecules are both expected to be located at the crystallite external surface of NaA, which internal network is characterized by small windows of diameters 0.4 nm. Samples were evacuated by freeze pump procedure up to 0.1 Pa and thermostated in the water or ethanol bath with accuracy ±1 K. The relative amount of DEC in the solid samples before and after evacuation procedure was controlled by ^{1}H NMR and DRIFT spectra.

Instrumentation and Data Analysis. ^{1}H NMR solid-state spectra were recorded at 300 MHz using a Bruker MSL 300 P spectrometer. Data were acquired with a spinning rate of 7 kHz under the magic angle condition (MAS) using a simple one radio frequency (RF) pulse sequence (Bloch decay), a RF field of 60 kHz and a relaxation waiting period of 20 s. TMS was used as an external reference for the chemical shifts. Spin−lattice relaxation times (T_1) were measured applying the standard inversion recovery sequence with an inter pulse delay in the 100 μs−20 s range. All the spectra were run at the probe head temperature (294 K).

For XPS analysis, a XSAM800 (KRATOS) X-ray Spectrometer operated in the fixed analyzer transmission mode was used, with a pass energy of 10 eV and a AlKα (1486.7 eV) X-ray source. Typical operating parameters were 13 kV and 10 mA. Samples were analyzed in ultrahigh vacuum with a base pressure in the sample chamber better than 10^{-5} Pa. Samples were analyzed at room temperature, with a takeoff angle of 90° relative to the surface. Spectra were collected and stored in 200 channels with a step of 0.1 eV, and 60 s of acquisition by sweep, using a Sun SPARC Station 4 with Vision software (Kratos). The photoelectron regions C 1s, O 1s, Na 1s, Al 2s and Si 2p were analyzed. For quantification purposes, the following sensitivity factors provided by Vision library were used: C 1s, 0.25; O 1s, 0.66; Na 1s, 2.3; Al 2s, 0.21; Si 2p, 0.27.

Infrared spectra of solid samples were recorded with Nicolet Impact 400D FTIR spectrometer in diffuse reflectance mode with 1 cm^{-1} resolution in the range 4000−500 cm^{-1}. Steady-state absorption spectra were obtained with a UV/vis Jasco-560 spectrophotometer.

The transient absorption spectra and decay kinetics of intermediates were recorded by laser photolysis technique with diffuse reflectance setup using the second harmonic (532 nm, beam diameter 1 cm, ≤50 mJ/cm^2, 3 ns pulse width) of Nd:YAG laser (Spectra-Physics, Quanta-Ray GCR-3) as an excitation source. In kinetic measurements,[29,30] the analyzing source was a 300 W xenon arc lamp (XM 300−5HS, ORC Lighting Products), and the detection used a F/3.4 monochromator (Applied Photophysics) and a R928 photomultiplier (Hamamatsu). The output signals were digitized by Tektronix 2430A digital oscilloscope (up to 150 MHz) and averaged in an IBM-compatible computer. In time-resolved absorption and luminescence spectra measurements,[31] a gated (Stanford Research System, Model D6535) intensified charge coupled device (ICCD, Oriel, Model Instaspec V, gate 2.2 ns) coupled to a fixed imaging compact spectrograph (Oriel, Model FICS 77440, 200−900 nm) was used as a detector.

Ground-state and transient reflectance of solid samples were analyzed in terms of Kubelka−Munk theory using eqs 1 and 2, respectively, where R and R' are diffuse reflectance from the

$$\Delta F = (1 - R)^2/2R - (1 - R')^2/2R' \quad (1)$$

$$\Delta F_t = (1 - R_t)^2/2R_t - (1 - R)^2/2R \quad (2)$$

surface of the samples with and without TPP, respectively, and R_t is the reflectance observed at time t after the laser pulse.[4−6] The values of ΔF and ΔF_t are proportional to the corresponding absorber concentration for optically thick samples with a homogeneous distribution of absorbers. The absorption of TPP at 532 nm in the solid samples was always smaller than 5%. Transient signal intensities were near saturation under experimental conditions and demonstrated almost total conversion of ground state into transient, implying the validity of Kubelka−Munk treatment for analysis of transient decays.[4−6]

Results

Solid-State ^{1}H NMR of *n*-Decanol Films on the NaA External Surface. Lines in ^{1}H solid-state NMR spectra are, in general, very broad and this is explained by the very strong homonuclear dipole−dipole interaction which scales with (HH distance)$^{-3}$, and consequently, wide-line static ^{1}H spectra are sensitive to molecular motion. Yet, in some cases useful information may be retained in ^{1}H MAS spectra. The ^{1}H solid-state MAS spectrum of NaA exibits a set of broad lines, with a full width at half-maximum (fwhm) of about 200 Hz and centered at 4.6 ppm (T_1 = 27 ms), which are attributed to the variety of OH groups of the zeolite. The presence of spinning sidebands indicates that the spinning rate has approached the line width in the static spectrum and that MAS at 7 kHz has

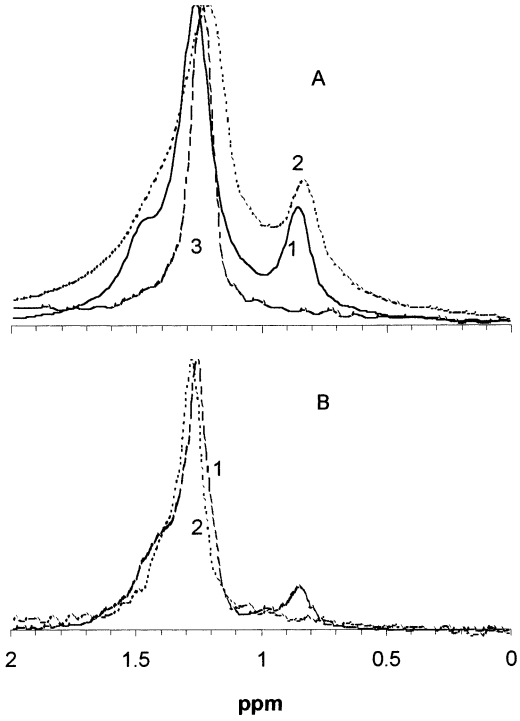

Figure 1. Normalized ^{1}H NMR solid-state spectra of solid samples of NaA (A) obtained in one pulse sequence experiments with 80 (1), 20 (2), and 5 μL/g (3) DEC and (B) obtained with the inversion recovery pulse sequence and an interpulse delay of 1 s with 80 (1) and 5 μL/g (2) DEC.

averaged dipolar interactions, thereby suppressing spin diffusion. Accordingly, for NaA samples the dominant HH distance appears to be of the order of the van der Waals HH distance (2.4 Å) because the corresponding dipole coupling constant is about 7 kHz. Moreover, the presence of asymmetric spinning sidebands reflects the electronic shielding anisotropy of the nuclei.

The addition of multilayer amounts of DEC to NaA solid samples results in the appearance of a somewhat broadened peak from α-CH_2 group (3.5 ppm, fwhm of about 40 Hz), relatively narrow aliphatic band from other CH_2 groups with maximum at 1.27 ppm, a shoulder at 1.46 ppm (β-CH_2 group), and a signal from the CH_3 fragment at 0.86 ppm (Figure 1A, plot 1). The OH band is masked by much stronger OH bands of NaA itself. The decrease of DEC amount from 20 to 5 monolayers is accompanied by the signal broadening of all aliphatic protons (Figure 1A, plot 2), and the α-CH_2 resonance becomes completely unresolved.

Further decrease of DEC concentration to one monolayer amount brings about the disappearance of signals from β-CH_2 and CH_3 groups and the width of the line at 1.25 ppm becomes two times smaller than that found in the thicker films (Figure 1A, plot 3). Similar features were observed for monolayers of other long-chain molecules on the solid support and, in conjunction with solid-state ^{13}C data, indicate a strong interaction of the headgroup with the surface, an extended *all-trans* chain conformation and the high molecular order along with large-amplitude motions about the chain long axes, with an increase of molecular mobility toward the unbound end.[32,33]

A detailed observation of T_1 weighted spectra, that is, spectra obtained with the inversion recovery (IR) pulse sequence and inter pulse delays shorter than $5T_1$, allowed the identification of less intense signals with shorter T_1. In the spectrum of DEC multilayer obtained with the IR pulse sequence and an inter

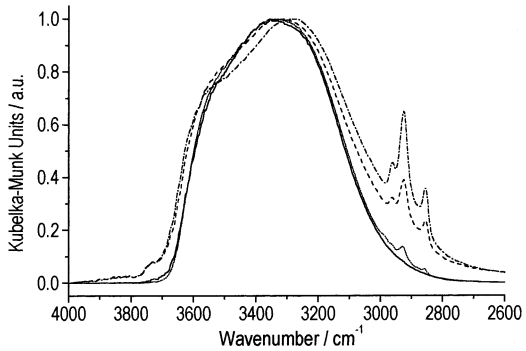

Figure 2. DRIFT spectra, in the range 2600−4000 cm^{-1}, of pure zeolite (—), and zeolite with increasing amounts of adsorbed decanol: close to the monolayer (••), intermediate (- −) and high (-•). The spectra were normalized to 1 at the maximum.

pulse delay of 1s, two signals at 1 and 0.86 ppm are assigned to CH_3 groups corresponding to different electronic environments (Figure 1B, plot 1). The values of T_1 could be measured for the resonances observed at 1.25 and 0.86 ppm: 685 and 960 ms, respectively. For comparison, the spectrum of DEC monolayer is also shown, which was obtained likewise with the IR pulse sequence and the same inter pulse delay (Figure 1B, plot 2); very small CH_3 signals are observed at about 1 ppm while the β-CH_2 signal appears as a shoulder at 1.36 ppm of the more intense resonance at 1.25 ppm. The value of T_1 for the signal at 1.25 ppm (250 ms) is significantly smaller than the corresponding value measured for multilayer. On the other hand, the T_1 value of the CH_3 group in the monolayer (800 ms) is similar to that obtained in the multilayer demonstrating the enhanced mobility of CH_3 terminal groups in DEC monolayer.

It is worthwhile mentioning that the ^{1}H solid-state NMR spectra of NaA samples with submonolayer amounts of DEC are similar to that of monolayer demonstrating the corresponding molecular organization within the islands of DEC on the external surface of zeolite particles.

Diffuse Reflectance Infrared Spectroscopy of *n*-Decanol Films on the NaA External Surface. This technique **(**DRIFT**)** was used to control the relative amounts of decanol in different samples. For this purpose, the spectra were normalized at the ν_{as}Si−O−Si band of the zeolite (at 984 cm^{-1}) and the relative intensities of the decanol strong bands at 2955 and 2928 cm^{-1} (assigned respectively to the $\nu_{as}CH_2$ and ν_sCH_2 modes) were taken as a measure of the decanol content. However, for very low concentrations (close to the monolayer), the spectral sensitivity was not enough to allow any conclusions regarding the orientation of the decanol chains. Nevertheless, when the decanol content increases, the different interactions among the OH groups may be qualitatively inferred from the modifications in the spectral region between 2600 and 4000 cm^{-1}, shown in Figure 2, normalized to the maximum of the νOH mode. This band centered at 3400 cm^{-1} involves the νOH of the zeolite's silanol groups, decanol and adsorbed water molecules. The zeolite and the sample with a decanol monolayer have similar band shapes (apart from the νCH_2 modes of decanol) and maximum absorption at ∼3356 cm^{-1}, which indicates that the OH groups from the few decanol molecules do not modify the hydrogen bonding between the adsorbed water molecules in the zeolite. This is not the case for samples with increasing decanol content: the νOH band becomes broader and clearly shows two main components, one shifted to lower wavenumbers (with maximum at 3311 and 3287 cm^{-1}, respectively, for intermediate and high decanol concentrations), and the other to higher wavenumbers (∼3600 cm^{-1}). Additionally, a fraction of free

OH groups remains, being responsible for the shoulder above 3700 cm^{-1}. Although quantitative conclusions could only be taken after a deconvolution of the band, it is possible to deduce that when a thicker layer of decanol is adsorbed on the zeolite, there is a larger variety of interactions between the OH groups, including those very similar to condensed decanol (the low-frequency component), decanol−water hydrogen bonding, and free OH groups.

XPS Studies of NaA Zeolite External Surface before and after Treatment with DEC. The XPS studies were performed with the sample of pure zeolite NaA after drying procedure and the sample of NaA with initial DEC amount of 10 μL/g. A large degassing takes place in the sample with DEC in the XPS chamber. The pressure of 10^{-5} Pa was achieved only after vacuum recovering during 24 h. Both samples presented a noticeable carbon (C 1s) signal but it was significantly larger in the sample with DEC (ratio C/Na = 0.8) than in the pure zeolite. The pressure behavior and the C 1s signal, suggest that some of the decanol molecules were chemically bound to the substrate but the majority were just physically adsorbed. The amount of residual chemically bound DEC molecules estimated from ^{1}H solid-state NMR spectra corresponded approximately to 1 μL/g. The external surface composition in aluminum, silicon, sodium, and oxygen is different from the bulky one (1:1:1:5). It is 1:0.89:1.25:4.58 for pure zeolite and 1:0.82:1.13:4.22 for sample with DEC. Therefore the chemical adsorption of DEC seems to occur preferentially at the surface oxygen centers bound to sodium and silicon atoms. This is compatible with an islandlike chemical adsorption. One other indirect evidence of the islandlike chemical adsorption rather than homogeneous one, comes from the degradation studies induced by the X-radiation on the samples. The surface content in carbon and in sodium increases while that in oxygen decreases with the irradiation time. Since the saturated hydrocarbon chains are very fragile under ionizing irradiation,[34] the increase in carbon signal may be due to a more effective covering of the zeolite external surface by the molecular pieces coming from the destruction of the islandlike domains of the long alkyl chains of DEC. A more homogeneous layer can produce a higher XPS signal than a similar or even larger amount of material arranged in an islandlike way.[35] The decrease of the oxygen signal may be attributed to the attenuation promoted by the covering of hydrocarbon debris. By contrast, the sodium signal should increase since the destruction of the DEC bound to the sodium centers results in the decrease of the corresponding attenuation effect.

Effect of Freezing on Ground State and Transient Absorption Spectra and Prompt fluorescence of TPP in Neat *n*-Decanol and in Films of *n*-Decanol on the NaA Surface. Figure 3A shows the diffuse reflectance spectra of TPP in the wavelength region of Soret band in frozen neat DEC in comparison with liquid DEC. Figure 3B presents the corresponding spectra of solid samples measured in DEC films. The freezing of both samples results in broadening (the half-width 11−12 nm and 14−20 nm at 295 and 260 K, respectively) and insignificant red shift (1−2 nm) of the Soret band which seems to reflect the transition of TPP from the homogeneous liquid phase to the heterogeneous medium. The broadening of the absorption bands in the inhomogeneous environment is a general phenomena which is observed, in particular, after adsorption onto the surface.[17,29,30,36] It is worthwhile mentioning that the half-width of Soret band in frozen DEC samples is significantly smaller than that found on dry surface of zeolites, silica and alumina (30 nm[17,29,30,37]). The microenvironment of TPP in frozen DEC matrix seems to be more homogeneous than that on dry surfaces. Figure 3C shows the effect of decreasing the decanol content at room temperature from bulk liquid to a monolayer film. No shift of the maxima is observed but the spectra becomes progressively broader, likely reflecting an increasing contribution of TPP interacting with the zeolite surface.

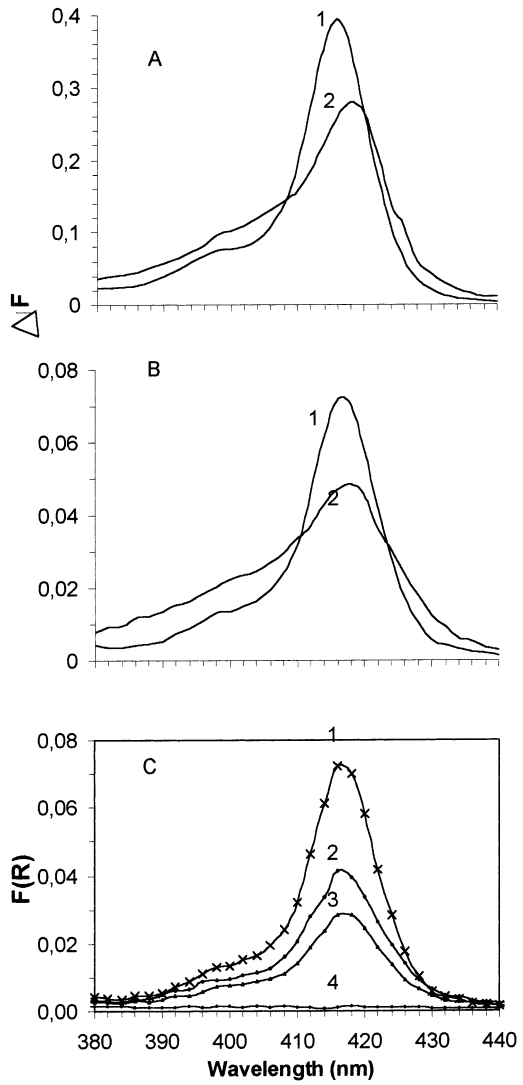

Figure 3. (A) The absorption (in terms of optical density) of the liquid (295 K) (1) and reflectance spectra (plotted using the differences in remission function ΔF) of frozen solid samples (260 K) of 10 μmol/L TPP in DEC. (B) Reflectance spectra of solid samples of 0.01 μmol/g TPP and 100 μL/g DEC on the external surface of NaA at 295 K (1) and 260 K (2). (C) Comparison of remission functions $F(R)$ of solid samples of 0.01 μmol/g TPP on the external surface of NaA with 100 μL/g DEC (1), 20 μL/g DEC (2), 5μL/g DEC (3), blank (4) at 295K.

Photoexcitation of TPP in solid and liquid samples results in transient absorption of ^{3}TPP characterized by differential spectra with strong bleaching at the wavelength of Soret band and maximum absorption near 440 nm.[17,18,26,27,38,39] The effect of DEC freezing is in the broadening of bleaching band near 420 nm which follows the corresponding changes in ground-state Soret absorption (see above).

A comparison of differential triplet−triplet absorption (measured immediately after the laser pulse $\Delta F_{t=0}$ at high laser fluence and small surface loading when transient signal intensities are in saturation) and initial TPP ground-state absorption at Soret

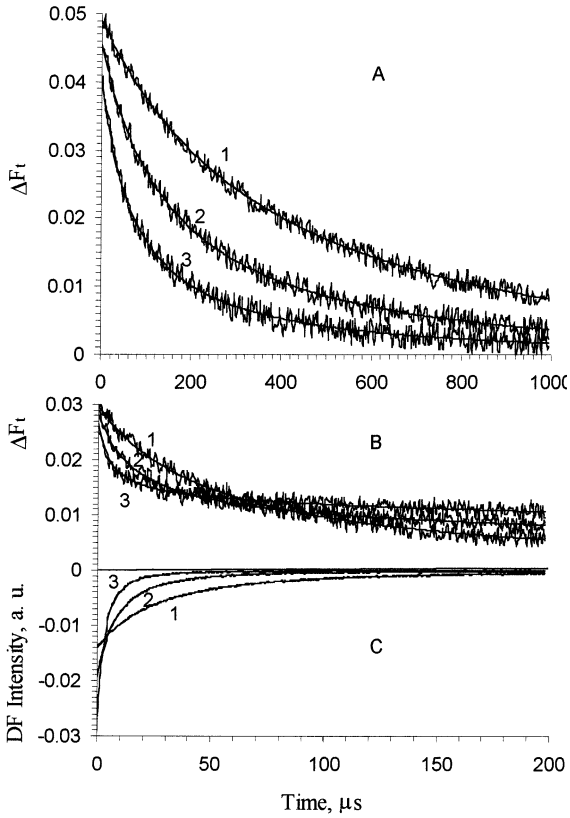

Figure 4. (A) Decays of the transient remission function change ΔF_t measured at 440 nm with deoxygenated samples of 10 μmol/L TPP in frozen DEC at 278 (1), 273 (2), and 260 K (3). (B) Decays of the transient remission function change ΔF_t measured at 440 nm with deoxygenated samples of NaA with 0.01 μmol/g TPP and coadsorbed 100 μL/g DEC at 295 (1), 273 (2), and 260 K (3). (C) Corresponding to (B) decays of transient emission at 650 nm. Lines are the best fitting to eq 3 (A), eq 3 with additional long-lived single-exponential component (B) and eq 4 (C).

band in both solid and liquid samples show, using literature values of corresponding extinction coefficients in solution,[38−41] that the efficiency of ground-state conversion to the triplet state corresponds to the ^{3}TPP quantum yield, φ_T (φ_T in the range 0.73−0.84 in different solvents has been reported[40−44]). It was assumed that $[T]_0 = 0.8$ [TPP] in solid and liquid samples at low TPP concentration and high laser fluence. The freezing of DEC has almost no effect on the ^{3}TPP quantum yield.

Only an insignificant effect of DEC freezing on the spectra, yield and lifetime (0.12 and 12.5 ns, respectively)[17] of TPP prompt fluorescence (PF) was found.[26] The parameters of TPP PF are almost temperature independent (within the experimental error 10%) both in solution and in the solid samples.

Effect of DEC Film Thickness on the Kinetics of TTA of TPP at Room Temperature. At room temperature, the decay kinetics of ^{3}TPP in evacuated solid systems DEC−NaA and in neat DEC with large local concentration of ^{3}TPP exhibit characteristic features of second-order decay (Figure 4B, curve 1). The transient is accompanied by DF with a spectral pattern (Figure 5) similar to that of PF and DF kinetics follows the square of ^{3}TPP concentration (Figure 4C, curve 1). It was shown already that in neat DEC and in DEC films on the NaA surface the kinetics of ^{3}TPP and DF is well described in terms of the classic kinetic scheme of TTA (Scheme 1).[17,26,27] Scheme 1 takes into account the ^{3}TPP self-decay (reaction 1, the value of k_0 in DEC has been estimated as 500 s^{-1});[17] the quenching by ground-state TPP (reaction 2, this process is negligible even for saturated solutions of TPP in DEC);[26] three possible channels of TTA

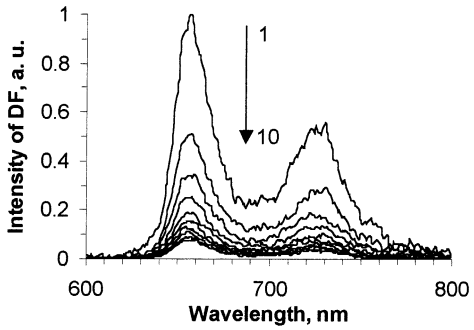

Figure 5. Time-resolved emission spectra of TPP 0.0005 μmol/g TPP in the solid NaA samples with 5 μL/g DEC measured at 295 K. Curve 1 was recorded 0.5 μs after the laser pulse, delay between curves 1−10 is 1 μs.

SCHEME 1

$$T \xrightarrow{k_0} S_0 \quad (1)$$

$$T + S_0 \xrightarrow{k_1} S_0 + S_0 \quad (2)$$

$$T + T \rightarrow \begin{cases} \xrightarrow{(1/9)k_2} {}^1(TT) \rightarrow S_0 + S_1 & (3) \\ \xrightarrow{(3/9)k_2} {}^3(TT) \rightarrow T + S_0 & (4) \\ \xrightarrow{(5/9)k_2} {}^5(TT) \rightarrow T + T & (5) \end{cases}$$

$$S_1 \rightarrow \begin{cases} \xrightarrow{k_{FL}} S_0 + h\nu & (6) \\ \xrightarrow{k_{IC}} S_0 & (7) \\ \xrightarrow{k_{IS}} T & (8) \end{cases}$$

via singlet (reaction 3), triplet (reaction 4), and quintet (reaction 5) intermediate complexes; and three pathways of first excited singlet-state decay: emission (reaction 6), internal conversion (reaction 7), and intersystem crossing (reaction 8). The integration of the system of equations corresponding to Scheme 1 in steady-state approximation ($d[S_1]/dt = 0$) gives eq 3 for ^{3}TPP concentration at time

$$[T]_t/[T]_0 = k^1\exp(-k^1t)/(k^1 + k_{obs}[T]_0(1 - \exp(-k^1t))) \quad (3)$$

t, $[T]_t$, where $k^1 = k_0 + k_1$[TPP] ([TPP] is the analytical concentration of TPP) and $k_{obs} = k_2(5 - \varphi_T)/9 - k_1$. The time dependence of DF intensity $I_{DF}(t)$ is described by eq 4, where

$$I_{TTADF}(t) = k_{FL}[S_1] = (1/9)\varphi_{FL}k_2[T]^2 \quad (4)$$

$\varphi_{FL} = k_{FL}/(k_{FL} + k_{IC} + k_{IS})$. The relative yield of DF, $Y_{DF}/Y_{PF} = \varphi_T/(5 - \varphi_T)$, where Y_{DF} and Y_{PF} are the total amounts of light emitted during DF and PF, respectively. The measured value of the $Y_{DF}/Y_{PF} = 0.19$ coincides exactly with that predicted by Scheme 1.[17,26,27]

A perfect fit of the ^{3}TPP decay kinetics to eq 3 was obtained for DEC solutions and films (Figure 4A, curve 1).[17,18,26,27] In multilayers of DEC on NaA external surface at temperatures above the melting point, the ^{3}TPP decay kinetics does not exhibit features of reactions in restricted geometries supporting the idea that TTA takes place in relatively homogeneous DEC microphase.[17,18]

The value of TTA rate constant related to the concentration of ^{3}TPP on the surface k_{obs}^S (calculated using measured value of $k_{obs}[T]_0$ and $[T]_0 = [^3TPP]_0$/surface area, where $[^3TPP]_0$ is the initial concentration of [^{3}TPP] related to the amount of NaA), decreases dramatically with the increase in the amount of DEC in solid sample (Figure 6A, plot 1) showing that the size of microreactor where TTA takes place correlates with the DEC volume. However, the corresponding plot differs significantly

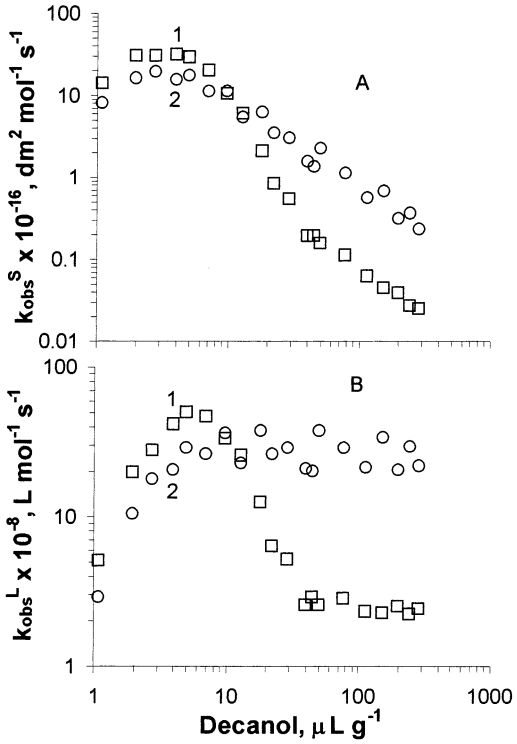

Figure 6. Plots of TTA rate constant related to the surface area k_{obs}^S (see text) (A) and that related to the DEC volume k_{obs}^L (see text) △ (B) on DEC concentration in the solid NaA samples measured at 295 (1, □) and 260 K (2, O).

from the linearity expected for homogeneous DEC microphase. In the samples with small amount of DEC, the k_{obs}^S value is not very sensitive to the DEC amount showing features of a surface reaction. Although the relatively fast TTA is observed also in the solid sample with small amount of DEC (1 μL/g or 1/4 of monolayers, estimated from the NMR spectra), one can see the tendency of k_{obs}^S decrease in samples with residual amount of DEC. It is worthwhile mentioning that the TTA does not occur on the dry NaA surface due to the very slow diffusion of adsorbed TPP molecules.[17,29,30]

The plot of TTA rate constant k_{obs}^L (calculated using measured value of $k_{obs}[T]_0$ with $[T]_0 = [^3TPP]_0/[DEC]$ on amount of DEC in solid sample) exhibits a built up when the amount of DEC decreases to the monolayer values (Figure 6B, plot 1). Further decrease of DEC amount results in decrease of k_{obs}^L.

In DEC solutions, it was found the value of $k_{obs} \sim 2 \times 10^8$ L mol^{-1} s^{-1} which corresponds to a value of k_2 very close to the diffusion-controlled limit.[17,26,27] The value of k_{obs}^L measured for solid samples with large DEC amount (≥10 monolayers) is similar to that found in neat DEC and it is independent of DEC content. For solid samples with one monolayer of DEC, the measured value of $k_{obs}^L \sim 5 \times 10^9$ L mol^{-1} s^{-1} is 25 times larger than that in neat DEC. Therefore, either the TPP mobility in DEC monolayer is much larger than that in the bulk DEC or TPP molecules are concentrated in some confined zone of monolayer, e.g., on the monolayer surface, or both.

Temperature Effect on the Kinetics of TTA of TPP in Neat *n*-Decanol and in DEC Films on the NaA Surface. The temperature effect on TTA in neat liquid DEC and in solid samples with large DEC amount (≥10 monolayers) at temperatures above mp is described by the Arrhenius law with an activation energy $E_a = 7 \pm 0.5$ kcal/mol (Figure 7, plots 3 and

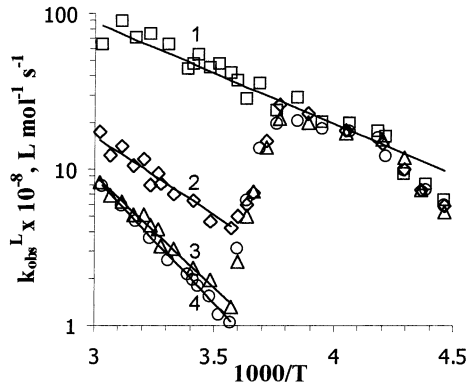

Figure 7. Temperature plots of TTA rate constant related to the DEC volume k_{obs}^L (see text) measured with 5 μL/g (1, □), 20 μL/g (2, ◊) and 100 μL/g (3, Δ) of DEC in the solid NaA samples. (4, O) Similar plot measured for neat DEC solution.

4), which is close to that of the viscous flow of DEC (6.3 kcal/mol) and also indicates that TTA is diffusion-controlled. The increase of k_{obs}^L with decrease of DEC film thickness is accompanied by the gradual decrease of E_a to 3 kcal/mol observed for solid samples with ≤2 monolayers of DEC (Figure 7, plot 1). This variation in E_a supports the idea that the TPP diffusion in DEC monolayers is faster than that in the bulk of DEC. On the other hand, if there is a lateral diffusion within the layer of terminal CH_3 group of DEC, the observed decrease of E_a can be compensated by the decrease in the corresponding entropy term.

A decrease in the temperature of the TPP solution in neat DEC to 279 K results in the phase transition with formation of a light-scattering layered polycrystalline material. This phase transition is accompanied by insignificant (within a factor of 2) increase of apparent k_{obs}. Further temperature decrease results in a significant gradual TTA acceleration (Figure 4A) and rise in apparent k_{obs} value which peaks at about 260 K and then decreases steeply (Figure 7, plot 4).[18,26,27] The decay kinetics of the most part of ^{3}TPP in neat frozen DEC remains second order with almost negligible contribution of the long-lived component related to trapped ^{3}TPP molecules (Figure 4A).

By contrast, the ^{3}TPP population falls into at least two distinct components after freezing of solid samples with DEC films (4B). A large fraction of ^{3}TPP exhibits fast second-order decay kinetics whereas the remainder disappears exponentially with the temperature independent first-order rate constant about 500 s^{-1}. The slow component seems to be related to TPP molecules trapped onto or in the vicinity of NaA surface. The contribution of slow component increases slightly with the decrease of temperature. The decay of "slow" ^{3}TPP population does not result in any distinguishable DF (Figure 4C).

The temperature plots for the TTA rate constant of the fast component obtained for solid samples with large amount of DEC (≥10 monolayers) are similar to the temperature plot found in neat DEC (Figure 7, plot 3), showing the rise up in local TPP concentration and/or mobility below mp By contrast, the expected phase transition in DEC monolayers has no effect on the decay of "fast" ^{3}TPP population. The corresponding temperature plot is of Arrhenius type in all temperature range studied with exception of very low temperatures (Figure 7, plot 1).

Effect of DEC Film Thickness on the Kinetics of TTA of TPP at Temperature 260 K. At low temperature, which corresponds to the maximum of TTA rate constant measured below the melting point, the plot of the TTA rate constant related to the NaA suface area k_{obs}^S on DEC amount in solid sample is

linear with unit slope with exception of samples with small amount of DEC (Figure 6A, plot 2). The TTA rate constant related to the DEC volume added to the sample k_{obs}^{L} is almost independent of the DEC amount for the samples with one or more DEC monolayers (Figure 6B, plot 2) showing the similarity of microreactors in the bulk of frozen DEC and within both liquid and frozen DEC monolayer. Therefore, one may assume that the frozen DEC bulk structure corresponds to the DEC monolayers with the TPP molecules localized in the vicinity of hydrophobic surfaces.

Discussion

Alcohol molecules are able to form multilayers adsorbed on the solid surfaces due to the self-association phenomena.[45−50] Scanning tunneling microscopy studies of DEC multilayers on solids showed complex structures with different types of domains, and molecular ordering occurring in the immediate vicinity of the substrate.[47] Numerous investigations on the structure of long-chain alcohols monolayers at liquid and solid hydrophilic surfaces revealed an orientation nearly vertical before and also after crystallization with appearance of long-range order at low temperatures.[21−25] The large advancing contact angles with water found for monolayers and multilayers with long-chain alcohols on silica and alumina based surfaces are typical of exposed methylene groups such as those in polyethylene-like surfaces.[49,51] A similar structure of DEC monolayers was expected on the highly hydrophilic external surface of NaA zeolite covered by the variety of hydroxyl groups and was confirmed by the NMR study. The hydrophobic TPP molecules appear to be localized in the hydrocarbon chains of DEC monolayers somewhere in the vicinity of the external monolayers surface with very mobile CH_3 groups. However, the significant screening effect of DEC monolayers found for the process of quenching of triplet and singlet excited states of TPP by O_2 implies that TPP molecules are not in the immediate gas/liquid interface.[17,18] The extraordinary large apparent rate of TTA found in organized DEC monolayers seems to be due to the increase in both TPP local concentration and diffusion, as is expected because of the small activation energy of TTA in monolayers and enhanced mobility of terminal CH_3 groups of DEC monolayer. The freezing of DEC monolayers on NaA external surface results in immobilization of approximately one-half of TPP molecules whereas the other part does not feel the phase transition demonstrating that the nature of reaction zone remains unchanged. The DEC monolayers are already organized at temperatures above the melting point, although conformational defects are somewhat reduced below the α-transition.[52]

The liquid to solid phase transitions are generally associated with dramatic retardation of diffusion controlled bimolecular processes due to the substantial restriction of the molecular translation mobility. However, the acceleration rather than retardation of bimolecular reactions between hydrophobic organic substances in aqueous solutions after freezing was reported for a number of systems.[53−56] It would appear natural that the dissolved organic molecules can be concentrated and aggregated in some defect regions in the course of crystallization. However, it has been questioned whether the concentration itself is enough to describe the freezing effect on hydrolytic reactions quantitatively.[57]

The displacement of dissolved molecules which do not fit the crystal lattice into the noncrystalline liquidlike microphase and the corresponding apparent acceleration of diffusion controlled bimolecular reactions seems to be not uncommon for polymorphous organic solvents. The temperature plots very similar to those presented in Figure 7 (plots 3 and 4) were obtained earlier by spin-probe ESR for the encounter frequency of N-oxyl radicals in *n*-decane, hexane, and benzene[28] as well as for TTA of TPP in benzene and aromatic alcohols.[27] In all systems studied, the apparent rate constant on the maximum in the temperature plots was more than 10 times above that in the liquid near the melting point. This temperature maximum was always observed 20−30 K below the melting point. This temperature plot implies that the apparent reaction volume and the probe translation mobility within it decrease with temperature and the maximum appears when both the local probe concentration and translation diffusion are optimal.

It is worthwhile mentioning that a formation of liquidlike microdomains in a partially polycrystalline matrix is not a result of freezing point depression due to the large organic probe local concentration. It still remains significantly smaller than that which is able to affect the melting point noticeably.[28] This conclusion is strongly supported by the temperature plots of the apparent TTA rate constant that are independent of TPP concentration in DEC, varied in the range of 0.001−0.1 mmol/L.[26] The observed temperature-dependent liquid-crystal equilibrium seems to be a specific property of some multilayered polycrystalline materials.

The question arises as to whether the solubility and mobility of dissolved molecules in this liquidlike microphase are similar to those in liquid solvent and if they are thermodynamically equilibrated. The magnitude of the effect suggests that it is possible to reach a very high local concentration of TPP in DEC (up to 0.1 mol/L, if the temperature dependence of TTA rate constant observed at temperatures above mp is extended to those below mp), where it is expected that TPP molecules should precipitate and aggregate, and the corresponding pronounced variations of absorption and fluorescence parameters should be observed. However, the prompt fluorescence spectrum, lifetime and quantum yield for TPP in frozen *n*-decanol are very similar to those observed in liquid solution. The assumption that the local concentration of TPP molecules increases significantly after DEC freezing is strongly supported by the studies of the DEC freezing effect on the singlet oxygen feedback induced DF which is due to the singlet oxygen mediated energy transfer between ^{3}TPP and observed in the presence of molecular oxygen.[18] It was found that the apparent oxygen mobility is much larger than that of TPP and it is not affected by DEC freezing but the efficiency of singlet oxygen feedback increases significantly due to the magnification of ^{3}TPP local concentration. However, the freezing effect on the corresponding rate constant was noticeably smaller than that on apparent rate of direct TTA. The comparison of direct and oxygen mediated TTA assumes the enhancement of both TPP mobility and local concentration. The unexpected large TPP solubility and diffusion in microreactors of frozen DEC can be attributed to both molecular organization and to the presence of crystalline surface. The broadening of TPP Soret absorption upon freezing neat DEC and DEC thick films support the idea that TPP molecules are in the immediate vicinity to some solid surface although in the last case the zeolite surface is involved as well.

The frozen system TPP−DEC seems to be relatively stable thermodynamically and does not change at least during several days, keeping the sample at 250 K. The direction and rate of the temperature change and the freezing have no pronounced effect on the corresponding temperature plots if the system is not frozen below 220 K.[18,26] In other systems, some hysteresis-like effects are usually expected especially if the starting temperature is below the β phase transition.[28] Frozen polycrys-

talline solutions may be thermodynamically unstable. For instance, similar temperature effects on kinetics of TTA of TPP have been found in the frozen solutions of TPP in *n*-dodecanol and *n*-hexadecanol immediately after freezing, but these systems were unstable in time showing the aggregation and immobilization of TPP molecules.[58]

The TTA kinetics of TPP in frozen neat solvents remains solely homogeneous although kinetics nonhomogeneity is the main characteristic feature of solid media due to the nonuniform spatial distribution of reactants and heterogeneous molecular environment.[18,26,27] However, both the kinetics of DF in frozen films of DEC on the zeolite surface which follows the TTA of a "fast" population of TPP triplets and the TTA kinetics in liquid and frozen organized DEC monolayer are not dispersed. Thus, one can assume that frozen DEC have a common organization feature with DEC monolayers, namely the layers with hydrocarbon-like external surface. The coincidence between extraordinary large TTA rate constant, related to the overall DEC volume, found in DEC monolayers and the corresponding rate constants of TTA in the bulk of frozen DEC supports the idea that, at least from the point of view of liquidlike microreactors, the frozen DEC consists of organized DEC monolayers. This type of organization seems to be consistent with common polymorphous crystalline forms (e.g., leaves or flakes) of amphiphilic organic substances.

Concluding Remarks

The kinetics of diffusion-controlled triplet−triplet annihilation of *meso*-tetraphenylporphyrin is used as a probe of molecular diffusion and organization of liquid and frozen thin *n*-decanol films adsorbed on the external surface of NaA zeolite in comparison with those in neat decanol. The apparent rate constant of TTA in DEC monolayers is found to be 1 order of magnitude larger than that in neat DEC or in the bulk of DEC multilayers on the surface at temperatures above the melting point of DEC. This effect is attributed not only to the concentration of TPP in the restricted part of monolayers but also to the enhanced diffusion of TPP in monolayers for which there are a number of indirect evidences.

The faster diffusion of probe molecules in organized organic monolayers compared to that in the liquid bulk is an unexpected result. However, one may conclude that since in the present system the organization of solvent molecules is controlled by the substrate surface, the external hydrocarbon area of monolayers may be an appropriate environment for a fast surface-like diffusion of dissolved molecules. The concept of fast lateral diffusion of TPP is supported by the small activation energy, enhanced mobility of terminal CH_3 groups in DEC monolayers, and by comparison of the freezing effect on parameters of direct and singlet oxygen mediated TTA. This concept is in agreement with more than 10 fold acceleration of TTA upon freezing of concentrated neat DEC solutions or DEC multilayers with large TPP concentration. Alternatively, it would be necessary to explain the 10 fold increase in solubility of TPP in liquidlike microreactors in frozen DEC. Nevertheless an enhanced solubility of TPP is also expected due to the specific nature of microreactors at the interfaces which differs significantly from that of a bulk liquid. The independence of the apparent bimolecular rate constant of TTA in the frozen systems on the amount of DEC in the film from one monolayer on the solid surface up to neat DEC defines the frozen DEC as organized monolayers with liquidlike hydrocarbon external surface.

Acknowledgment. This work was supported by POCTI/1999/QUI/35398 and in part by FCT (Programatic funds), and by the Russian Foundation for Basic Research (00-03-32190). P.P.L. thanks CQE for the award of an Invited Scientist Fellowship.

List of Abbreviations

DEC, *n*-decanol
DF, delayed fluorescence
k_{obs}^{S}, apparent rate constant of triplet−triplet annihilation related to the surface area
k_{obs}^{L}, apparent rate constant of triplet−triplet annihilation related to the decanol volume in the solid sample
PF, prompt fluorescence
S_0, singlet ground state
S_1, first singlet excited state
T, triplet excited state
TPP, *meso*-tetraphenylporphyrin
TTA, triplet−triplet annihilation
φ_T, triplet state quantum yield
φ_{FL}, fluorescence quantum yield

References and Notes

(1) Ulman, A. *An Introduction to Ultrathin Organic Films*; Academic Press: Boston, 1991.
(2) Decher, G. *Science* **1997**, *277*, 1232.
(3) Zhang, J.; Chi, Q.; Kuznetsov, A. M.; Hansen, A. G.; Wackerbarth, H.; Christensen, H. E. M.; Andersen, J. E. T.; Ulstrup, J. *J. Phys. Chem.* **2002**, *106*, 1131.
(4) Oelkrug, D.; Uhl, S.; Wilkinson, F.; Willsher, C. J. *J. Phys. Chem.* **1989**, *93*, 4551.
(5) Oelkrug, D.; Gregor, M.; Reich, S. *Photochem. Photobiol.* **1991**, *54*, 539.
(6) Wilkinson, F.; Worrall, D. R.; Williams, S. L. *J. Phys. Chem.* **1995**, *99*, 6689.
(7) Kopelman, R.; Parus, S.; Prasad, J. *Phys. Rev. Lett.* **1986**, *56*, 1742.
(8) Khairutdinov, R. F.; Levin, P. P.; Costa, S. M. B. *Langmuir* **1996**, *12*, 714.
(9) Cano, M. L.; Cozens, F. L.; Garcia, H.; Scaiano, J. C.; Marti, V. *J. Phys. Chem.* **1996**, *100*, 18152.
(10) Cozens, F. L.; Regimbald, M.; Garcia, H.; Scaiano, J. C. *J. Phys. Chem.* **1996**, *100*, 18165.
(11) Sykora, M.; Kincaid, J. R.; Dutta, P. K.; Castagnola, N. B. *J. Phys. Chem. B* **1999**, *103*, 309.
(12) Smalley, J. F.; Feldberg, S. W.; Wool, S. H. *J. Phys. Chem.* **1989**, *93*, 2570.
(13) Coutinho, P. J. G.; Costa, S. M. B. *Chem. Phys.* **1994**, *182*, 399.
(14) Khairutdinov, R. F.; Hurst, J. K. *J. Phys. Chem. B* **1999**, *103*, 3682.
(15) Baranyai, P.; Gangl, S.; Grabner G.; Knapp, M.; Kohler G.; Vidoczy T. *Langmuir* **1999**, *15*, 7577.
(16) Partee, J.; Frankevich, E. L.; Uhlhorn, B.; Shinar, J.; Ding, Y.; Barton, T. J. *Phys. Rev. Lett.* **1999**, *82*, 3673.
(17) Levin, P. P.; Costa, S. M. B. *J. Photochem. Photobiol. A* **2001**, *139*, 167.
(18) Levin, P. P.; Costa, S. M. B. *Int. J. Photoenergy* **2002**, *4*, 161.
(19) Rabe J. P.; Buchholz S. *Science* **1991**, *253*, 424.
(20) Wu, X. Z.; Ocko, B. M.; Sirota, E. B.; Sinha, S. K.; Deutsch, M.; Cao, B. H.; Kim, M. W. *Science* **1993**, *261*, 1018.
(21) Zakri, C.; Renault, A.; Rieu, J.-P.; Vallade M.; Berg, B. *Phys. Rev. B.* **1997**, *55*, 14163.
(22) Vysotsky, Yu. B.; Bryantsev, V. S.; Fainerman V. B.; Vollhardt D.; Miller R. *J. Phys. Chem. B* **2002**, *106*, 121.
(23) Dai, Y.; Evans, J. S. *J. Phys. Chem. B* **2001**, *105*, 10831.
(24) Mugele, F.; Baldelli, S.; Somorjal, G. A.; Salmeron M. *J. Phys. Chem. B* **2000**, *104*, 3140.
(25) Franz V.; Butt H.-J. *J. Phys. Chem. B* **2002**, *106*, 1703.
(26) Levin, P. P. *Russ. Chem. Bull.* **2000**, *49*, 1831.
(27) Levin, P. P. *Dokl. Phys. Chem.* **2000**, *374*, 187.
(28) Mil, E. M.; Kovarskii, A. L.; Vasserman, A. M. *Izv. Akad. Nauk SSSR, Ser. Khim.* **1973**, *10*, 2211.
(29) Levin, P. P.; Costa, S. M. B.; Ferreira, L. F. V.; Lopes, J. M.; Ribeiro, F. R. *J. Phys. Chem. B* **1997**, *101*, 1355.
(30) Levin, P. P.; Costa, S. M. B.; Lopes, J. M.; Serralha, F. N.; Ribeiro, F. R. *Spectrochim. Acta A.* **2000**, *56*, 1745.
(31) Ferreira, L. F. V.; Ferreira, M. R. V.; Oliveira, A. S.; Branco, T. J. F.; Prata, J. V.; Moreira J. C. *Phys. Chem. Chem. Phys.* **2002**, *4*, 204.
(32) Badia A.; Gao W.; Singh S.; Demers L.; Cuccia L.; Reven L. *Langmuir* **1996**, *12*, 1262.

(33) Badia A.; Lennox, R. B.; Reven L. *Acc. Chem. Res.* **2000**, *33*, 475.
(34) Rei Vilar, M.; Schott, M.; Pfluger, P. *J. Chem. Phys.* **1990**, *92*, 5722.
(35) Neves, P.; Arronte, M.; Vilar, R.; Botelho do Rego, A. M. *Appl. Phys. A* **2002**, *74*, 191.
(36) Hoffmann, K.; Marlow, F.; Caro, J. *Zeolites* **1996**, *16*, 281.
(37) Levin, P. P.; Costa, S. M. B. *Chem. Phys.* **2000**, *263*, 423.
(38) Pekkarinen, L.; Linschits, H. *J. Am. Chem. Soc.* **1960**, *82*, 2407.
(39) Rodriguez, J.; Kirmaier, C.; Holten, D. *J. Am. Chem. Soc.* **1989**, *111*, 6500.
(40) Tran-Thi, T. H.; Lipskier, J. F.; Maillard, P.; Momenteau, M.; Lopez-Castillo, J.-M.; Jay-Gerin, J.-P. *J. Phys. Chem.* **1992**, *96*, 1073.
(41) Kikuchi, K.; Kurabayashi, Y.; Kokubun, H.; Kaizu, Y.; Kobayashi, H. *J. Photochem. Photobiol. A* **1988**, *45*, 261.
(42) Gradyushko, A. T.; Sevchenko, A. N.; Solovyov, K. N.; Tsvirko, M. P. *Photochem. Photobiol.* **1970**, *11*, 387.
(43) Pineiro, M.; Carvalho, A. L.; Pereira, M. M.; Gonsalves, A. M. d′A. R.; Arnaut, L. G.; Formosinho, S. J. *Chem. Eur. J.* **1998**, *4*, 2299.
(44) Gurinovich, G. P.; Jagarov, B. M. *Luminescence of Crystals, Molecules and Solutions*; Plenum Press: New York, 1973; p 196.
(45) Waksmundzki, A.; Leboda, R.; Suprynowicz, Z. *Chem. Anal.* **1972**, *17*, 1223.
(46) Markowski, W.; Soczewinski, E.; Czapinska, K. L. *Pol. J. Chem.* **1983**, *57*, 1329.
(47) Magonov, S. N.; Wawkuschewski, A.; Cantow, H. J.; Liang, W.; Whangbo, M. H. *Appl. Phys. A: Solids Surf.* **1994**, *59*, 119.
(48) Matyjasiak, A.; Stroka, J.; Galus, Z. *Electroanalysis* **1996**, *8*, 987.
(49) Fagerholm, H. M.; Rosenholm, J. B.; Horr, T. J.; Smart, R. S. *Colloids Surf. A* **1996**, *110*, 11.
(50) Forlan, G. M.; Coll, J. *Interface Sci.* **2001**, *242*, 477.
(51) Iler, R. K. *The Chemistry of Silica*; John Wiley: New York, 1979.
(52) Sefler, G. A.; Du, Q.; Miranda, P. B.; Shen, Y. R. *Chem. Phys. Lett.* **1995**, *235*, 347.
(53) Grant, N. H.; Clark, D. E.; Alburn, H. A. *J. Am. Chem. Soc.* **1961**, *83*, 4476.
(54) Prusoff, W. *Biochim. Biophys. Acta* **1963**, *68*, 302.
(55) Butler, A. R.; Bruice, T. C. *J. Am. Chem. Soc.* **1964**, *86*, 313.
(56) Kano, K.; Zhou, B.; Hashimoto, S. *J. Phys. Chem.* **1985**, *89*, 3748.
(57) Bruice, T. C.; Butler, A. R. *J. Am. Chem. Soc.* **1964**, *86*, 4104.
(58) Levin, P. P.; Costa, S. M. B. Unpublished results.